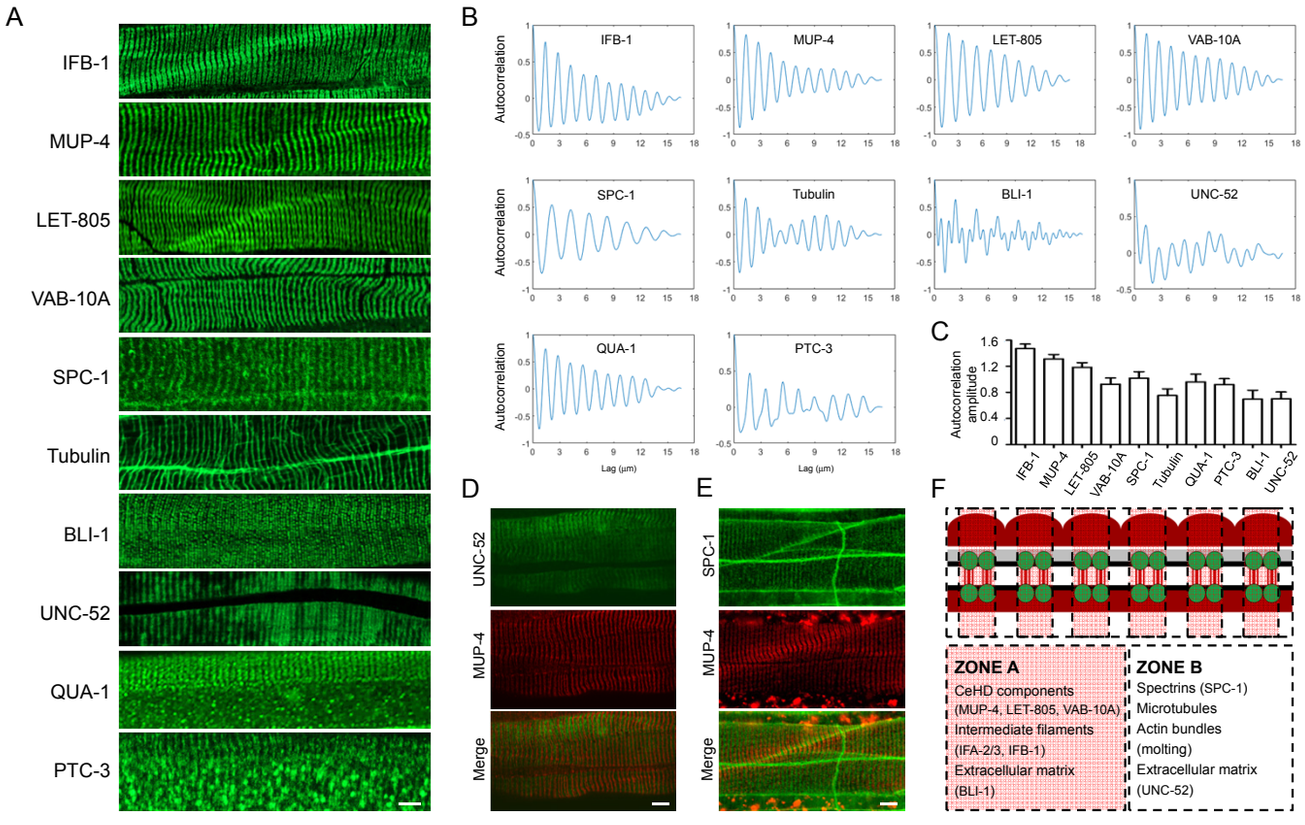

Figure S1. The periodic subcellular structures in the *C. elegans* epidermis share a common framework. **(A)** Representative confocal images showing the periodical patterns of intermediate filaments (IFB-1::GFP), microtubules (anti-tubulin), α-spectrin (SPC-1::GFP), spectraplakin (VAB-10A::GFP), apical and basal CeHDs (MUP-4::GFP and LET-805::GFP), apical and basal ECM (BLI-1::GFP and anti-UNC-52), as well as Hedgehog family ligand and receptor (QUA-1::GFP and PTC-3::GFP) in the *C. elegans* epidermis at the young adult stage. **(B)** The periodicity of periodically arranged subcellular structures in the *C. elegans* epidermis represented by autocorrelation analysis. **(C)** The average amplitude of autocorrelation analysis for different periodic subcellular structures. Error bars represent the mean±s.e.m. The quantification results show that the CeHD components display higher periodicity than other subcellular structures in the *C. elegans* epidermis. **(D)** Double-labeling of UNC-52 and MUP-4 by immunostaining in the young adult epidermis. **(E)** Double-labeling of SPC-1::GFP and MUP-4::mCherry in the young adult epidermis. **(F)** Diagram showing the relative positions of periodically arranged subcellular structures in the C. *elegans* epidermis based on previous publications and figure S1D-E. Scale bars, 5 μm.

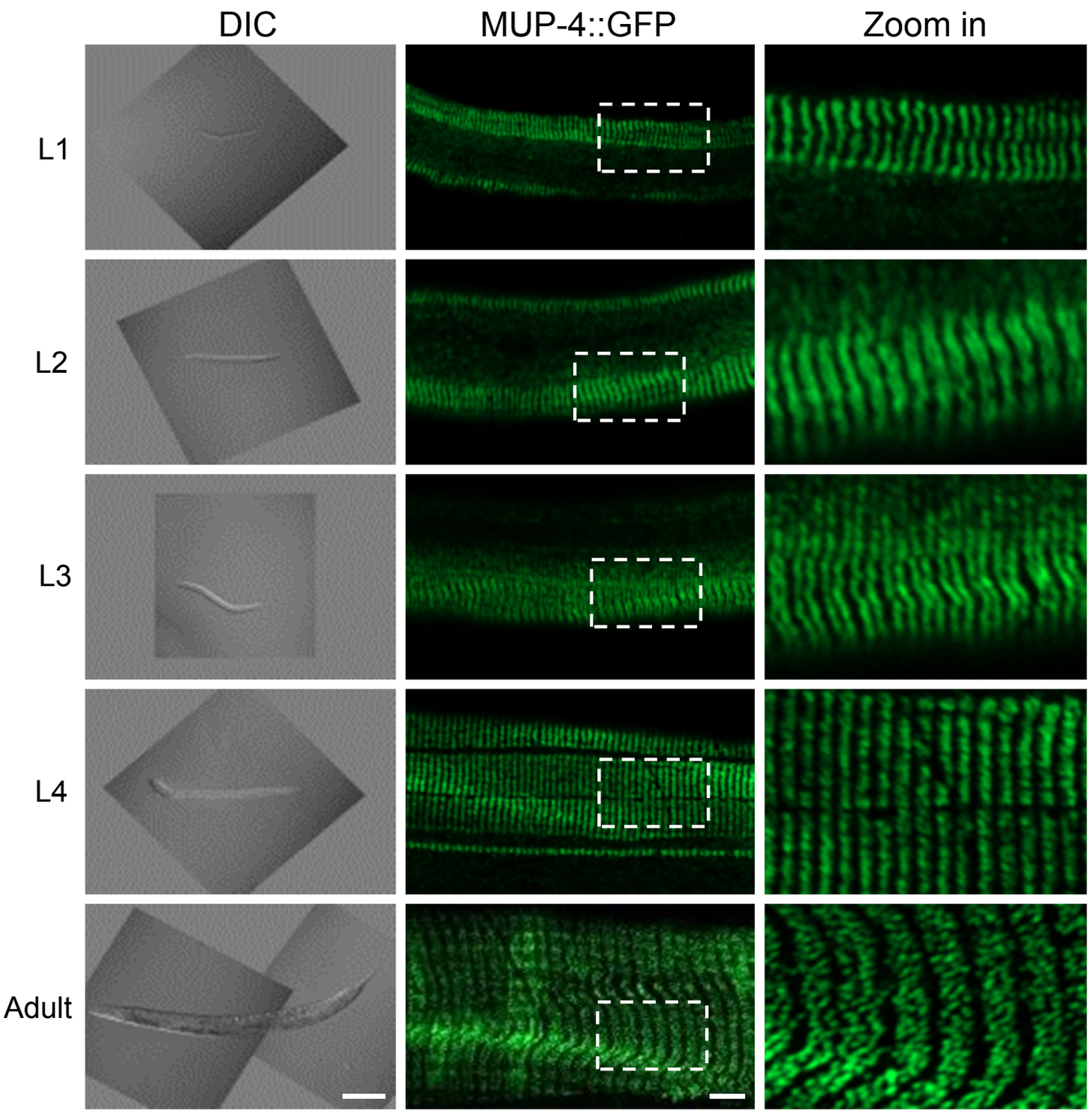

Figure S2. The reorganization of apical CeHDs during post-embryonic development.

Representative confocal images and corresponding bright-field images showing MUP-4::GFP localization in live animals at L1-4 larvae and adult stages. Boxed areas are enlarged on the right. Scale bars, 5 µm.

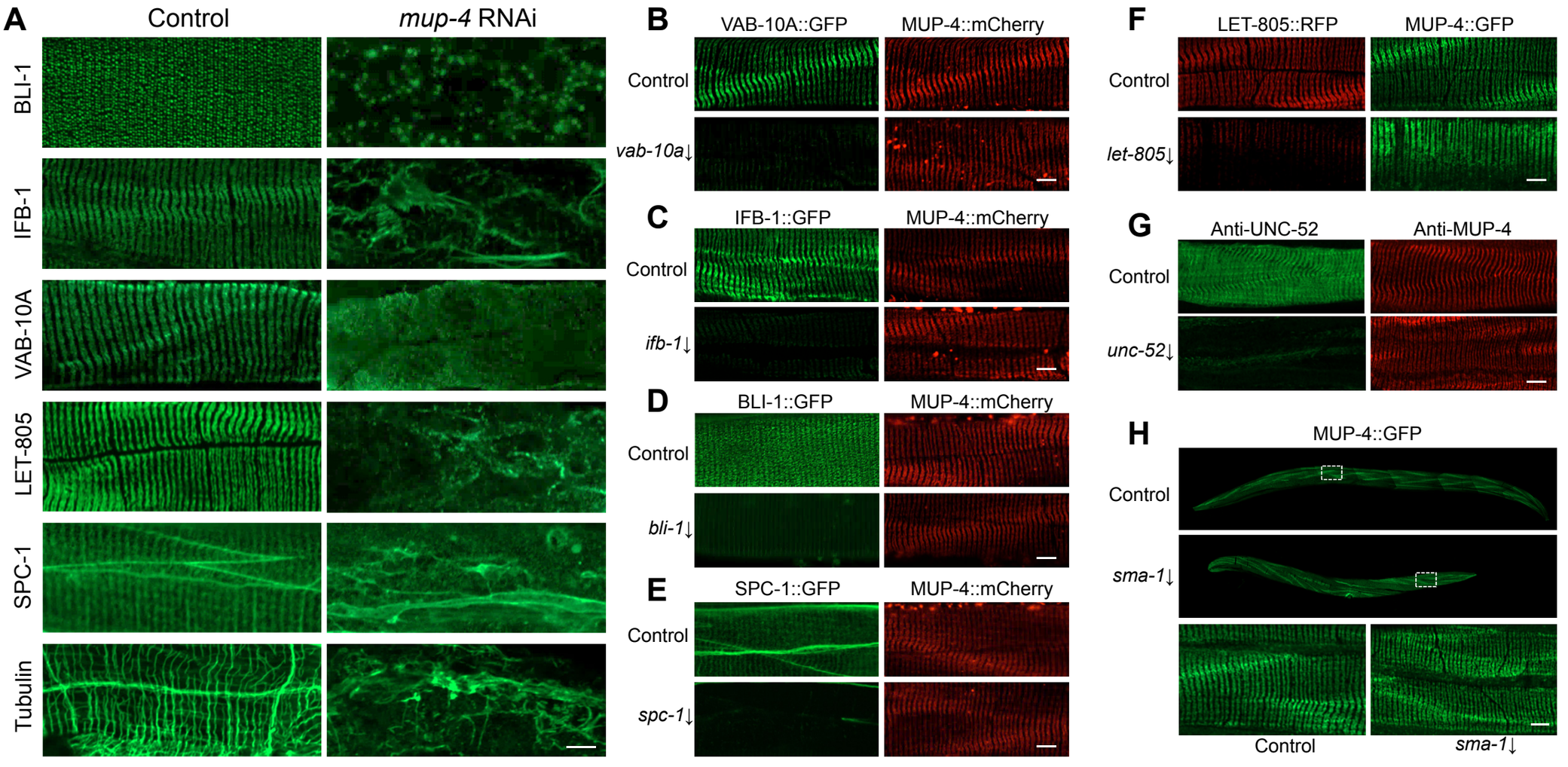

Figure S3. The apical CeHDs are required for maintaining the periodic patterns of other subcellular structures.

(A) Localization patterns of BLI-1::GFP, IFB-1::GFP, VAB-10A::GFP, LET-805::GFP, SPC-1::GFP and microtubules (anti-tubulin) in wildtype young adult epidermis treated with *mup-4* RNAi clone targeting 141bp-1111bp of *mup-4* transcript. The specificity of *mup-4* RNAi was confirmed by similar phenotypes caused by RNAi clone targeting 141bp-1111bp and 3857bp-4958bp of *mup-4* transcript (see figure 3). **(B-G)** The knock-down efficiency of *let-805, vab-10a, ifb-1, spc-1, bli-1* and *unc-52* RNAi in young adult epidermis was confirmed by fluorescent reporters of BLI-1::GFP, IFB-1::GFP, VAB-10A::GFP, LET-805::GFP, SPC-1::GFP and anti-UNC-52 immunostaining. MUP-4::GFP or MUP-4::mCherry reveals that the striped CeHD patterns were not affected by inactivation of these genes. **(H)** The knock-down efficiency of *sma-1* RNAi was confirmed by composite confocal images showing **t**he phenotype of significantly shortened body length of *sma-1* RNAi–treated young adult compared with control. MUP-4::GFP reveals that the striped patterns were not affected by loss of *sma-1* function. Boxed regions are enlarged below. Scale bars, 5 μm.

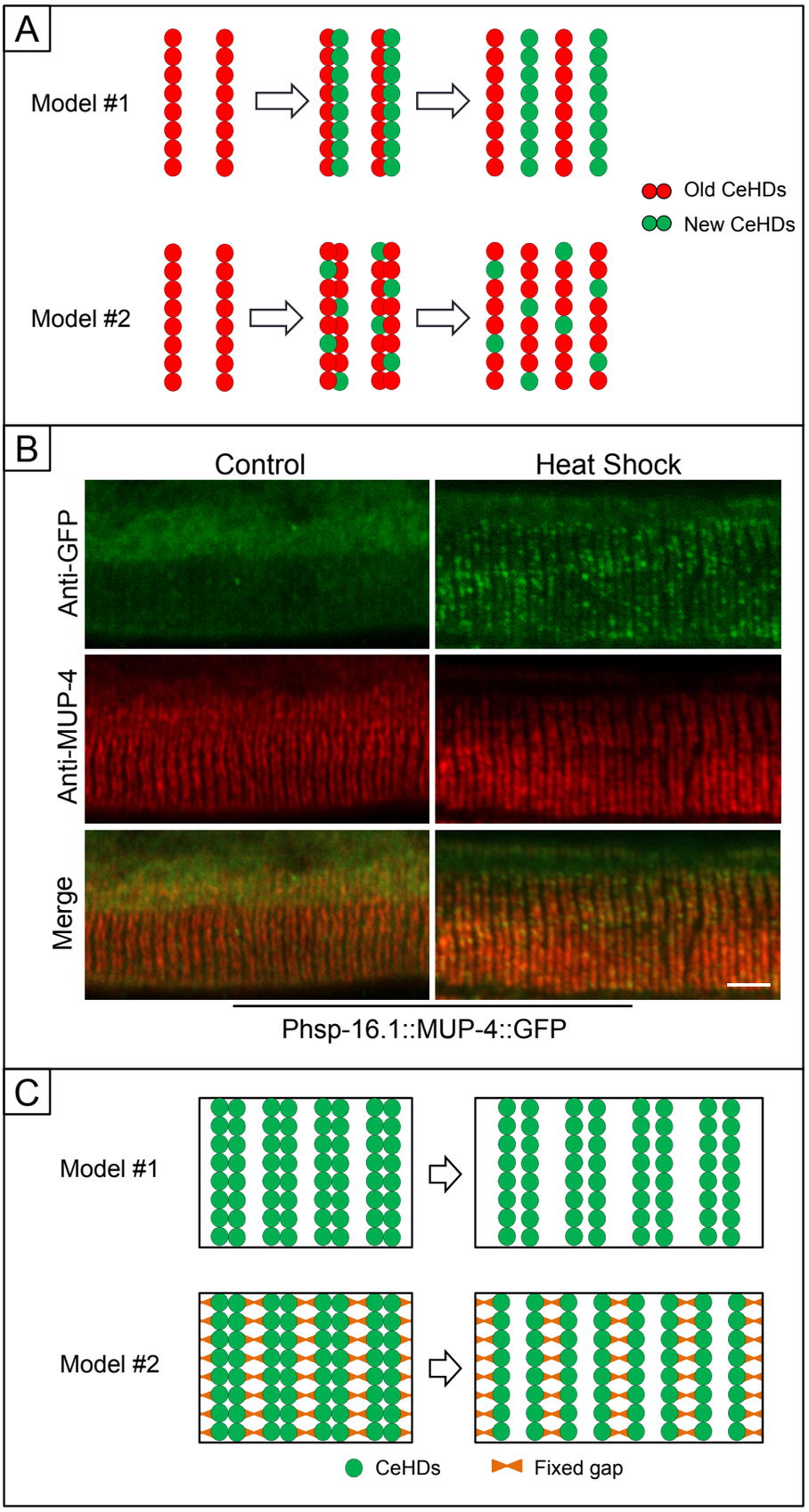

Figure S4. The CeHDs stripe thickening and separation process.

(A) Hypothetic models for the mechanisms underlying CeHD stripe thickening. There are potentially two ways to achieve stripe thickening: the new CeHD units (green) could either use the old stripes (red) as a template to align into a brand new stripe, or they could be randomly inserted into the old stripes (**(B)** Double-labeling of newly formed MUP-4 (green, anti-GFP) and total MUP-4 (red, anti-MUP-4) in L3 larvae carrying Phsp-16.1::MUP-4::GFP transgene treated with or without heat shock at 34℃ for 30min. Scale bar, 5 μm. **(C)** Hypothetic models for the mechanisms underlying CeHD stripe separation. Model 1: The distance between adjacent CeHD stripe doublets are not fixed. The stripes separate by passive expansion as the cell grows, therefore the gaps between the stripe doublets are always wider than the fissure within the stripe doublets. Model 2: The distance between adjacent CeHD stripe doublets are fixed and maintained by physical links. As the cell expands, the gaps between the stripe doublets remain the same width whereas the fissure within the stripe doublets greatly increases.

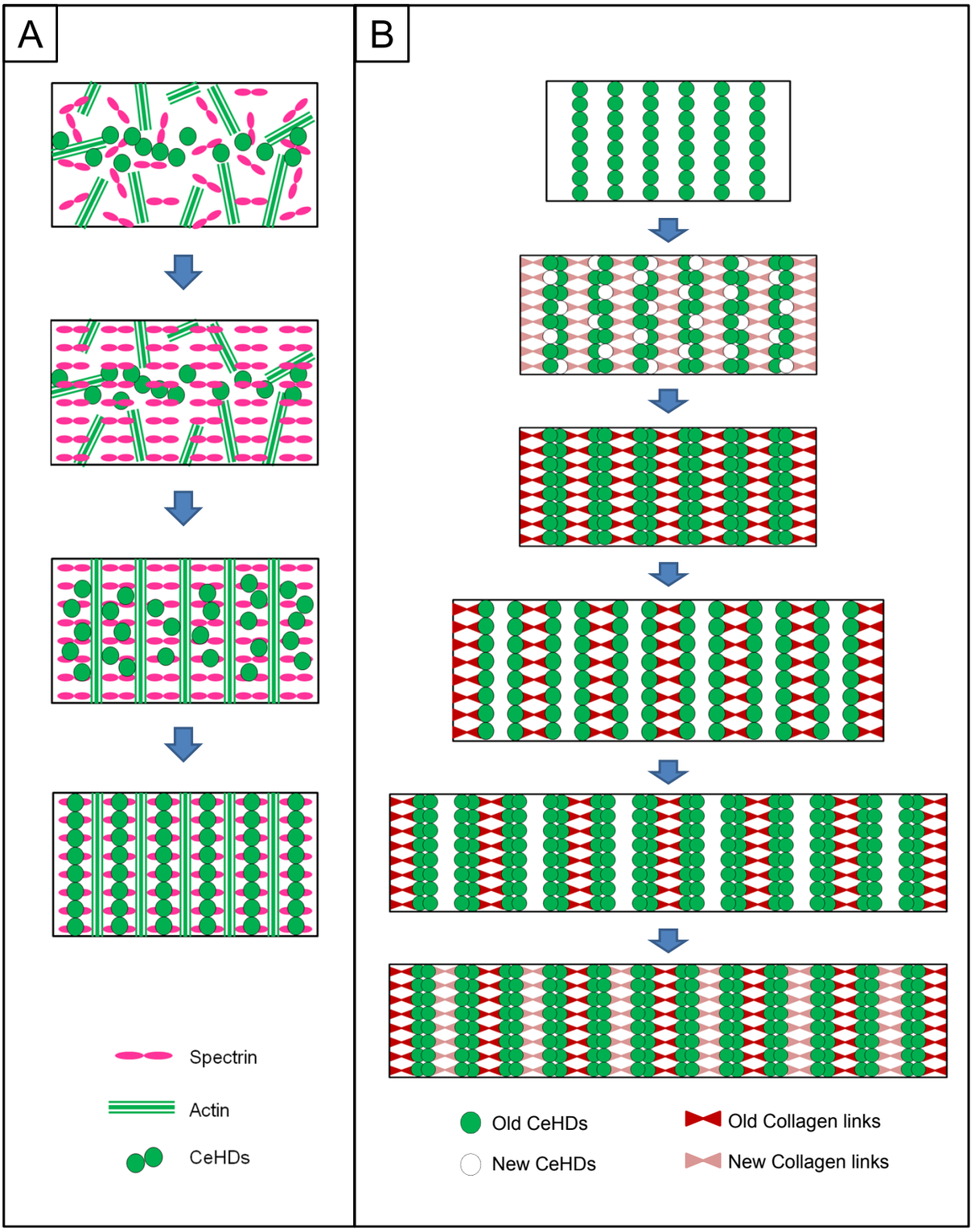

Figure S5. The initiation and synchronized reorganization of the periodic patterns in the *C. elegans* epidermis.

Diagrams showing the current models of the intracellular periodic pattern formation during embryogenesis (A) and the stripe duplication process during post-emybronic development (B) in the *C. elegans* epidermis.